

## AN ANALYSIS OF THE INTERACTION BETWEEN TWO WHEELS AND A DISCRETELY SUPPORTED RAIL

<sup>1</sup>. DEPARTMENT OF RAILWAY VEHICLE, UNIVERSITY POLITEHNICA OF BUCHAREST, ROMANIA

**ABSTRACT:** The paper herein presents an analysis of the interaction between two wheels and a rail (ballasted track) due to the small-scale undulation of the rail rolling surface. To this end, a new model of the periodic support of the rail that improves the prediction of the rail response for both low and high frequencies is used. It is shown the fact that the vibrations of the two wheels are coupled due to the bending waves which travel along the rail between them. However, these waves are strongly attenuated for three particular frequency ranges - the stop zones. When the vibration frequency is out of the stop zones, the wheel/rail contact force has two components - one comes from the wheel it self and other one is given by the influence of the conjugate wheel. In this way, the amplitude of the contact force versus frequency has a succession of peaks and deeps depending on the velocity and wheels base.

**KEYWORDS:** wheel, rail, discrete support, bending waves, frequency-domain analysis

### INTRODUCTION

The small-scale undulations (roughness) of both rolling surfaces—the wheel and the rail—are among the common causes of the wheel/rail vertical vibration. The study of the vibration generated by a wheel while rolling on a rail in the presence of the small-scale undulations is critical in predicting the short-pitch rail corrugation [1, 2] and the rolling noise [3, 4].

Usually, the wheel-rail vibration behavior is studied using a model in which only a single wheel is present. This is not the case in practice, where multiple wheels roll on the rail [5].

Simulating the wheel/rail vibration behavior with high accuracy depends mainly on the track model which is crucial from this perspective. Using the previous models [6, 7], two frequency ranges still remain critical. On the one hand, the rail receptance is underestimated at low frequencies (below 50 Hz). On the other hand, for the frequencies that are situated within the 'pinned-pinned' frequency range, the rail receptance at mid span is over-estimated.

The issue of the wheel/rail interaction may be solved in two different ways—using either the model of a 'moving irregularity' between a stationary wheel and rail, or the model of a 'moving wheel' along the rail. The model of the moving irregularity is much easier to use and it is currently utilized for the frequency-domain analysis [5, 8].

In this paper, applying the 'moving irregularity' model, the frequency-domain analysis of the interaction between two wheels and a discretely supported rail is presented. In order to obtain more accurate results, overcoming the above difficulties, the track model suggested in the references [9 - 11] is used.

### MECHANICAL MODEL

It considers the case of two wheels running with constant velocity  $V$  on a discretely supported rail as can be viewed in Figure 1. Such model is used to study the interaction between a railway vehicle and ballasted track at frequencies much higher than the natural frequencies of the vehicle, over 20 Hz [12, 13]. This fact allows neglecting the influence of the vehicle suspension and the inertia of the suspended masses of the vehicle (car body and bogie). On the other hand, both vehicle and track are considered symmetric structures and the wheels vibration of a particular bogie is not influenced by the wheels vibration of other bogie.

Track model consists of a discretely supported rail on rail pad, sleepers, ballast and subgrade [9-11]. The rail is considered a uniform infinite Timoshenko beam and the sleepers are assumed as rigid bodies. In addition, the inertial effect due to the ballast bed enters the equation. Three directional Kelvin-Voigt systems are in use to model the visco-elastic feature of the rail pad and ballast, and a mixed Kelvin-Voigt/Maxwell system for the subgrade.

For frequency-domain analysis, the moving irregularity model is adopted, the wheels are considered fixed above the rail, and the roughness is 'drawn' between wheels and rail in the opposite direction of wheels travel real.

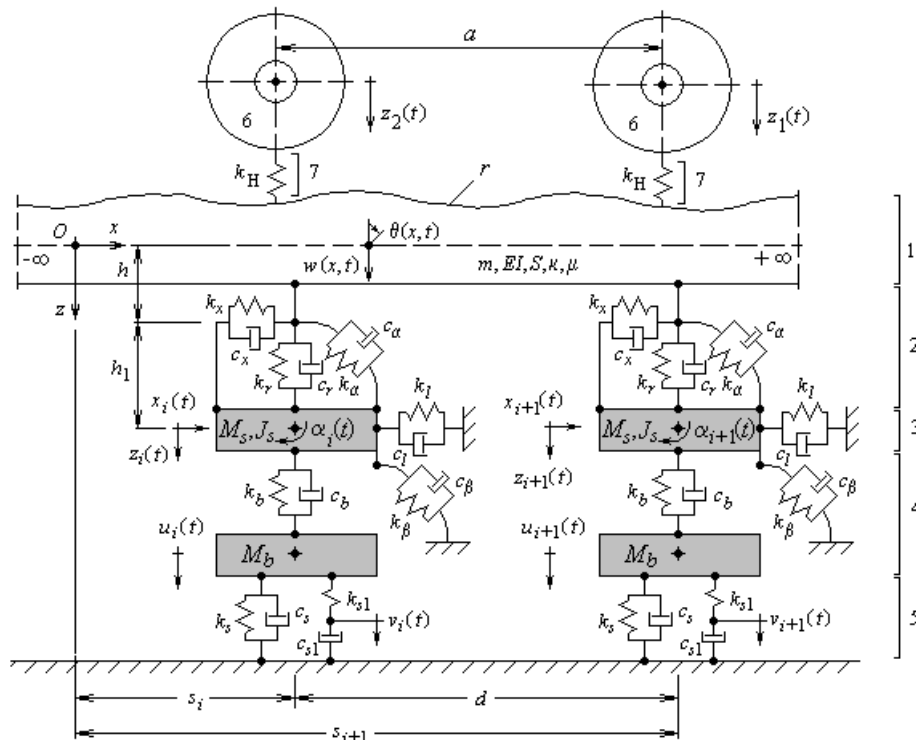


Figure 1. Mechanical model of two wheels/rail interaction: 1. rail; 2. rail pad; 3. sleeper; 4. ballast; 5. subgrade; 6. wheel; 7. wheel/rail contact.

The contact model between wheels and rail is based on the Hertz's theory and a linear approximation is performed so that the elastic constant is given as

$$k_H = \frac{3}{2} \sqrt[3]{Q_0 C_H^2} \quad (1)$$

where  $Q_0$  is the static load and  $C_H$  - the Hertzian constant.

The displacements of the two wheels are  $z_1$  and  $z_2$ , and the rail displacement below the wheels is noted  $w_1$  and respectively  $w_2$ .

Wheels/rail contact equation takes the form

$$\delta_i(t) = z_i(t) - w(x_i, t) - r(x_i) = \Delta Q_i / k_H, \text{ cu } i = 1, 2 \quad (2)$$

where  $\delta_i$  stands for the wheel/rail deflection,  $r_i$  represents the rail irregularity below the wheel  $i$ ,  $\Delta Q_i$  is the dynamic component of the wheel/rail contact force due to the rail irregularity and  $x_i$  - the position of the  $i$  wheel.

The harmonic steady-state behavior requires the complex variable for rail irregularity

$$\bar{r} = \bar{r}_0 \exp(ikx) = \bar{r}_0 \exp(ikVt) = \bar{r}_0 \exp(i\omega t), \quad (3)$$

where  $\bar{r}_0$  is the complex amplitude of the irregularity,  $k$  - wavenumber of the rail irregularity,  $\omega$  - angular frequency and  $i^2 = -1$ .

Considering the initial phase zero below the front wheel, the irregularity below the rear wheel has the form

$$\bar{r}_1 = \bar{r}(x_1) = r_0 \exp(i\omega t); \quad \bar{r}_2 = \bar{r}(x_2) = r_0 \exp[i\omega(t - a/V)]. \quad (4)$$

The complex variables describing the harmonic steady-state behavior are as follows

$$\bar{z}_{1,2}(t) = \bar{z}_{1,2} \exp(i\omega t); \quad \bar{w}(x_{1,2}, t) = \bar{w}(x_{1,2}) \exp(i\omega t); \quad (5)$$

$$\bar{\delta}_{1,2}(t) = \bar{\delta}_{1,2} \exp(i\omega t); \quad \Delta \bar{Q}_{1,2}(t) = \Delta \bar{Q}_{1,2} \exp(i\omega t). \quad (6)$$

Using the Green's functions method, the rail displacement can be calculated via the convolution theorem

$$\bar{w}_i = \bar{w}(x_i) = \int_{-\infty}^{\infty} G(x_k, \xi) \sum_{k=1}^2 \Delta \bar{Q}_k \delta(\xi - x_k) d\xi = G(x_i, x_1) \Delta \bar{Q}_1 + G(x_i, x_2) \Delta \bar{Q}_2, \quad i = 1, 2, \quad (7)$$

where  $G(x, \xi)$  is the Green's function of the rail.

The Green's function of the rail  $G(x, \xi)$  gives the rail response in the  $x$  section caused by a unit harmonic force by a particular angular  $\omega$  frequency, occurring in the  $\xi$  rail's section. Actually, this function is the rail's receptance and it is represented by a complex number. The Green's function of the rail can be calculated following the similar method described in a previous paper [14].

Displacement of the wheel  $i$  has the form

$$\bar{z}_i = -\bar{\alpha}_w \Delta \bar{Q}_i, \tag{8}$$

where the  $\alpha_w$  wheel's receptance is given by the equation

$$\bar{\alpha}_w = -\frac{1}{\omega^2 M_w}. \tag{9}$$

Inserting equations (8) and (9) in the contact equation (7), the following equations result

$$\begin{aligned} (\bar{\alpha}_w + \bar{\alpha}_r + \bar{\alpha}_H) \Delta \bar{Q}_1 + \bar{\alpha}_{ra} \Delta \bar{Q}_2 &= -\bar{r}_1; \\ \bar{\alpha}_{ra} \Delta \bar{Q}_1 + (\bar{\alpha}_w + \bar{\alpha}_r + \bar{\alpha}_H) \Delta \bar{Q}_2 &= -\bar{r}_2, \end{aligned} \tag{10}$$

where 
$$\bar{\alpha}_H = \frac{1}{k_H}, \bar{\alpha}_r = G(x_1, x_1) = G(x_2, x_2), \bar{\alpha}_{sa} = G(x_1, x_2) = G(x_2, x_1). \tag{11}$$

Generally speaking, it has to be mentioned the fact that  $G(x_1, x_1) \neq G(x_2, x_2)$ . However, when the distance between the wheels equals the sleeper bay multiplied by an integer number, it reads  $G(x_1, x_1) = G(x_2, x_2)$ . On the other hand, it reads always  $G(x_1, x_2) = G(x_2, x_1)$  due to the Betty's principle - the Green's functions are symmetrical.

The wheel/rail contact forces result from the equations (10)

$$\Delta \bar{Q}_1 = \frac{\bar{\alpha}_{ra} \bar{r}_2 - \bar{\alpha}_{wr} \bar{r}_1}{\bar{\alpha}_{wr}^2 - \bar{\alpha}_{ra}^2}; \Delta \bar{Q}_2 = \frac{\bar{\alpha}_{ra} \bar{r}_1 - \bar{\alpha}_{wr} \bar{r}_2}{\bar{\alpha}_{wr}^2 - \bar{\alpha}_{ra}^2}, \tag{12}$$

where 
$$\bar{\alpha}_{wr} = \bar{\alpha}_w + \bar{\alpha}_r + \bar{\alpha}_H. \tag{13}$$

From equations (3) and (4), the roughness below the rear wheel can be written as follows

$$\bar{r}_2 = \bar{r}_1 \exp(-i\omega a / V) = \bar{r} \exp(-i\omega a / V), \tag{14}$$

This equation shows that the rear wheel excitation is delayed with the phase of  $\omega a / V$ .

Under these circumstances, the contact force-roughness response can be calculated using the following equations

$$\frac{\Delta \bar{Q}_1}{\bar{r}} = \frac{\bar{\alpha}_{sa} \exp(-i\omega a / V) - \bar{\alpha}_{rs}}{\bar{\alpha}_{rs}^2 - \bar{\alpha}_{sa}^2}; \frac{\Delta \bar{Q}_2}{\bar{r}} = \frac{\bar{\alpha}_{sa} - \bar{\alpha}_{rs} \exp(-i\omega a / V)}{\bar{\alpha}_{rs}^2 - \bar{\alpha}_{sa}^2}. \tag{15}$$

**NUMERICAL APPLICATION**

In this section, numerical simulations are carried out using the model presented in the previous sections for two wheels/rail interaction. The sleeper bay of 0.6 m and the wheels base of 1.8 m have been considered. The value of wheels base correspond to the one of the freight wagons. The other parameters of the track model can be found in references [9-11].

Figure 2 shows the rail receptance for two particular cases, first, when the harmonic force is applied above sleeper and second, when the harmonic force acts between sleepers, at mid span. The receptance at loading point is displayed and also the receptance at the distance of 1.8 m from the loading point. As it can notice, the rail receptance decreases up to 50 Hz as being influenced by the ballast and the subgrade, according to the measurement results delivered by Knothe and Wu [15].

Within the range of the mid frequencies, the rail receptance diagram presents the specific aspect of a system with two degree of freedom:

- there are two resonance frequencies (at about 120 and 480 Hz) and,
- an anti-resonance frequency between

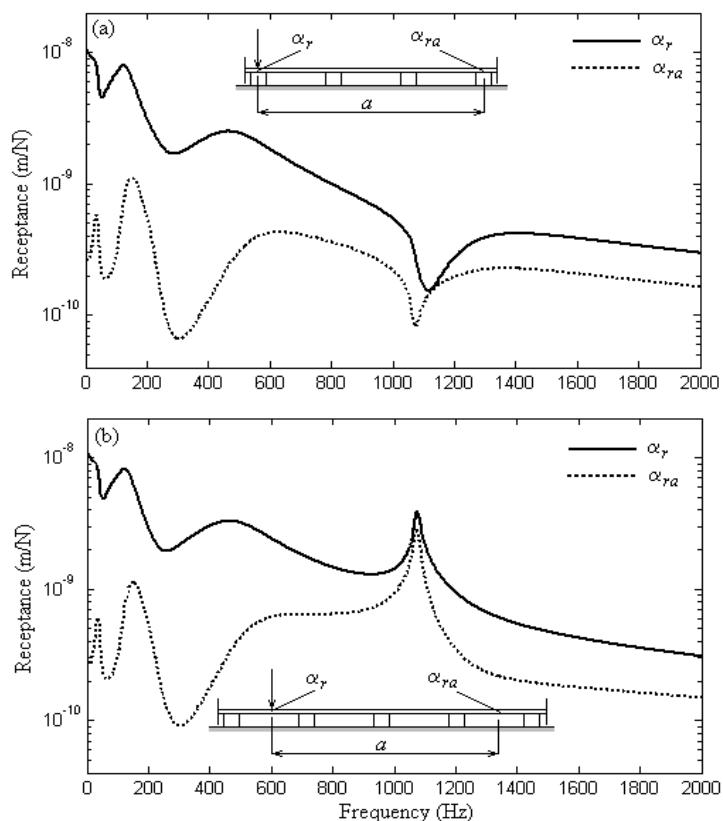


Figure 2. Rail receptance: (a) above sleeper; (b) at mid span.

them (at approximately 240 Hz). At higher frequency, the dynamic response of the rail is dominated by the effect of the periodic support, namely the pinned-pinned resonance that occurs when the rail is excited at mid span and the wavelength of the bending waves is twice the span (around 1075 Hz). If the harmonic force is applied above the sleeper, then the rail dynamics exhibits an anti-resonance behavior (1120 Hz).

Rail response at a particular distance from the loading point, in this case 1.8 m, allows pointing out how the bending waves propagate along the rail. There are three frequency zones when the bending waves are much attenuated - the so-called stop zones. The first stop zone occupies the range of the very low frequencies 0 - 20 Hz. The second stop zone is situated between 60 and 100 Hz, and the third stop zone is around the frequency of 300 Hz. The bending waves of high frequency propagate very well, especially at the pinned-pinned resonance frequency when the emerging point is at mid span.

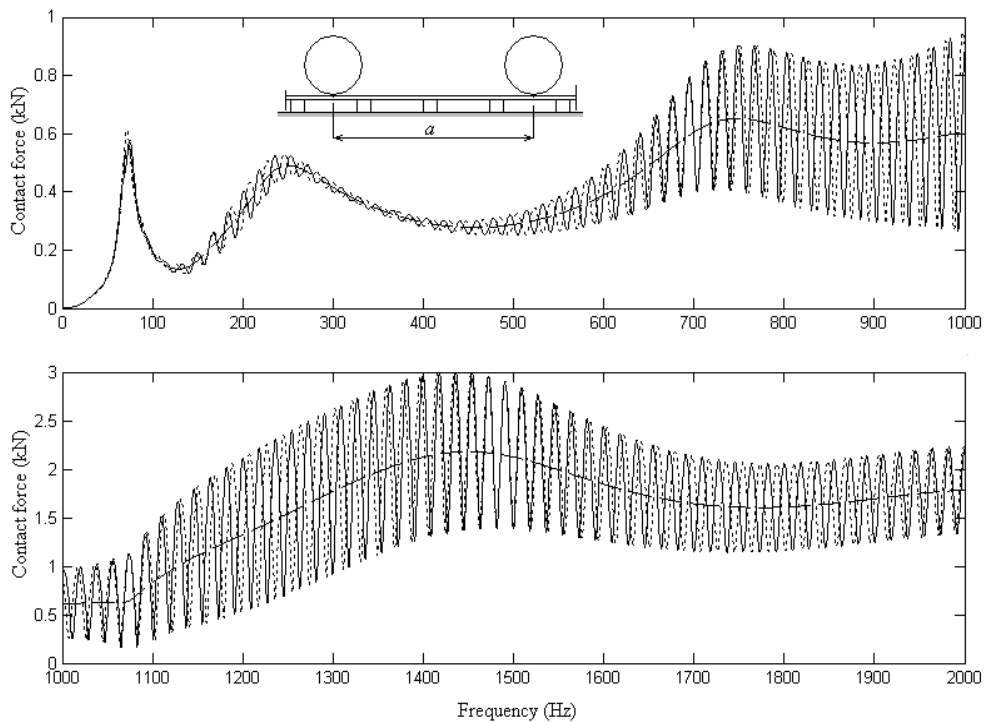


Figure 3. Wheel-rail contact forces when the wheels are at mid span: —,  $Q_1$ ; ···,  $Q_2$ , - - -,  $Q$ .

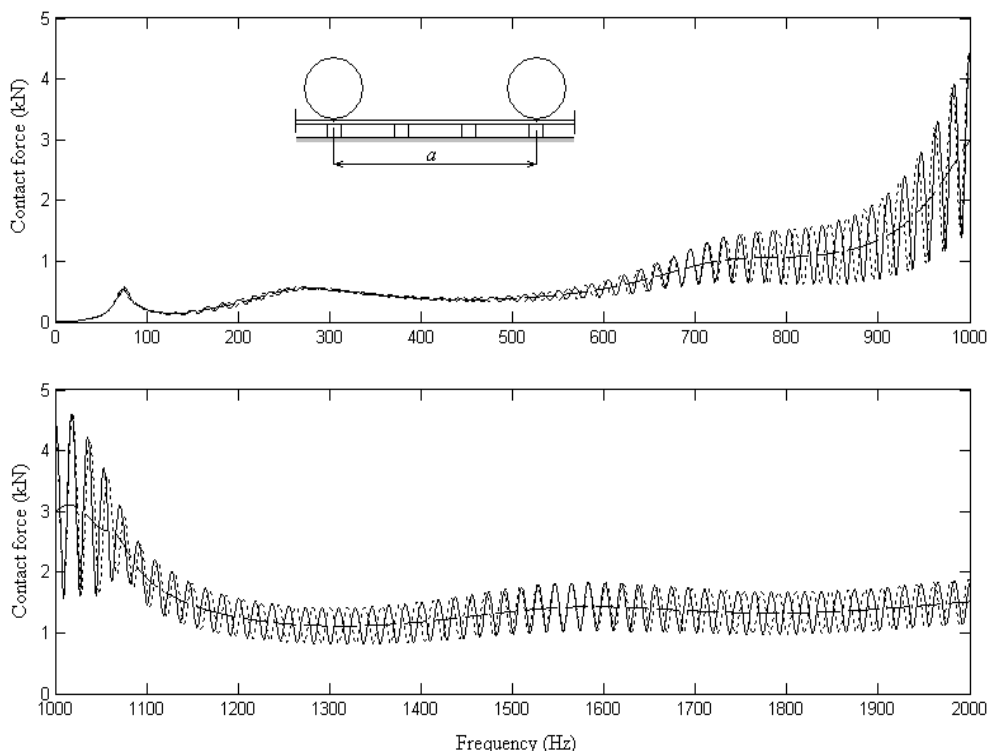


Figure 4. Wheel-rail contact forces when the wheels are above sleepers: —,  $Q_1$ ; ···,  $Q_2$ , - - -,  $Q$ .

Figure 3 shows the wheel-rail contact forces  $Q_1$  and  $Q_2$  when the two wheels are placed at mid span and the roughness amplitude is  $1 \mu\text{m}$ . The mass of each wheel is 750 kg and the wheels velocity is 120 km/h. Also, the wheel/rail contact  $Q$  due to a wheel alone at mid span is displayed. The values of contact forces  $Q_1$  and  $Q_2$  oscillate around the  $Q$  value and this aspect becomes significant for frequencies between the first and second stop zone and at frequencies higher than 500 Hz. This fact is the results of two causes. On the one hand, each contact force has a variable component depending on frequency due to the presence of the conjugate wheel (the rear wheel for the front wheel and viceversa). In this way, the contact force exhibits peaks and deeps at every  $\Delta v = 18 \text{ Hz}$  ( $\Delta v = V/a$ ). On the other hand, these peaks and deeps become effective only when the bending waves can propagate from the conjugate wheel, i.e. the frequency is not within a stop zone.

Some features can be identified from figure 3: the peak of the wheel/rail resonance with the frequency of 60 Hz, and the maximum of contact force corresponding to the rail's anti-resonance at the frequency of 240 Hz. Also, the two zones dominated by the anti-resonant response (120 Hz and respectively 450 Hz) can be explained by the two rail's resonances. Further on, other two maximum responses can be signalized at 730 and 1450 Hz due to the relative low receptance of the rail.

Finally, figure 4 presents the correspondent results for the case when the wheels are above sleepers. Comparing with the previous results, the contact forces have a similar variation up to 700 Hz. It has to observe the very high values about 1000 Hz due to the mixed influences of the decreasing of the rail's receptance and the contact elasticity.

## CONCLUSIONS

In this paper, the interaction between two wheels and rail has been analyzed using a new model for the rail periodic support. The rail is modeled as an infinite Timoshenko beam and the model of the periodic support consists of two three-directional Kelvin-Voigt systems for the rail pad and the ballast, and a mixed Kelvin-Voigt/Maxwell system for the subgrade. Also, the inertia of the sleeper and the ballast block are taken into account. The theoretical results obtained by means of this model show a good agreement with the results from the measurements for an extended frequency range, particularly at low frequencies (0-50 Hz) and at the pinned-pinned resonance frequency.

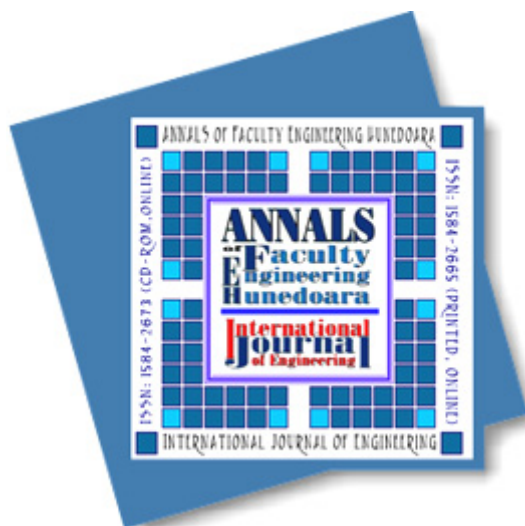
The interaction between the two wheels and rail is conditioned by the bending waves which travel along the rail between the two wheels. However, there are several frequency ranges in which the banding waves are strongly attenuated - the stop zones.

The wheel/rail contact force has two components, respectively one comes from the wheel it self and other one is given by the influence of the conjugate wheel. Because of this influence, the amplitude of the contact force versus frequency has a succession of peaks and deeps depending on the velocity and wheels base. The contact force component due to the conjugate wheel becomes effective when the frequency of the bending waves is not in a stop zone.

## REFERENCES

- [1.] Nielsen, J.C.O., Lundén, R., Johansson, A., T. Vernersson, Train-track interaction and mechanisms of irregular wear on wheel and rail surfaces, *Vehicle System Dynamics* 40, 3-54, 2003.
- [2.] Oostermeijer, K.H., Review on short pitch rail corrugation studies, *Wear* 265, 1231-1237, 2008.
- [3.] Remington, J.P., Wheel/rail rolling noise: what do we know? What don't we know? Where do we go from here? *Journal of Sound and Vibration* 120, 203-226, 1988.
- [4.] Thompson, D.J., Jones, C.J.C., A review of the modelling of wheel/rail noise generation, *Journal Sound and Vibration* 231, 519-536, 2000.
- [5.] Wu, T.X., Thompson, D.J., Vibration analysis of railway track with multiple wheels on the rail, *Journal of Sound and Vibration* 239, 69-97, 2001.
- [6.] Zhai, W.M., Wang, K.Y., Lin, J.H., Modelling and experiment of railway ballast vibrations, *Journal of Sound Vibration* 270, 673-683, 2004.
- [7.] Nielsen, J.C.O., High-frequency vertical wheel-rail contact forces-validation of a prediction model by field testing, *Wear* 265, 1465-1471, 2008.
- [8.] D.J. Thompson, Wheel-rail noise generation, part IV: contact zone and results, *Journal of Sound and Vibration* 161, 447-466, 1993.
- [9.] Mazilu, T, Dumitriu, M, Tudorache, C, Sebeşan, M., On vertical analysis of railway track vibrations, *Proceedings of the Romanian Academy Series A Mathematics Physics Technical Sciences Information Science* 11, 156-162, 2010.
- [10.] Mazilu, T, Dumitriu, M, Tudorache, C, Sebeşan M., New method for calculating response of a periodic structure due to moving loads, *Proceedings of the Romanian Academy Series A Mathematics Physics Technical Sciences Information Science* 11, 340-346, 2010.
- [11.] Mazilu, T, Dumitriu, M, Tudorache, C, Sebeşan I., Using the Green's functions method to study wheelset/ballasted track vertical interaction, *Mathematical and Computer Modelling* 54, 261-279, 2011.

- [12.] Dumitriu, M., Modelling of vehicle-track system to study the vertical vibrations, *Annals of the “Constantin Brâncuși” University of Târgu Jiu*, issue. 4, 2012, pp. 53-64.
- [13.] Dumitriu, M., On the dynamic vertical wheel-rail forces at low frequencies, *Mechanical Journal Fiability and Durability*, issue supplement no. 1, 2012, pp. 11-17.
- [14.] Mazilu, T., Green’s functions for analysis of dynamic response of wheel-rail to vertical excitation, *Journal of Sound and Vibration* 306, 31-58, 2007.
- [15.] Knothe, K., Wu, Y., Receptance behaviour of railway track and subgrade, *Archive of Applied Mechanics* 68, 457-470, 1998.



**ANNALS of Faculty Engineering Hunedoara**



**- International Journal of Engineering**

**copyright © UNIVERSITY POLITEHNICA TIMISOARA,  
FACULTY OF ENGINEERING HUNEDOARA,  
5, REVOLUTIEI, 331128, HUNEDOARA, ROMANIA  
<http://annals.fih.upt.ro>**